Experimental Study on a Fast Tracking and Smooth Constrained Motion Controller for Robot Arms

E.C. Dean-León, L.G. García-Valdovinos
Mechatronics Division, CINVESTAV-IPN
AV. IPN 2508, Sn P. Zacatenco, México, D.F.,7300. México
{*edean, lgarcia*}*@cinvestav.mx*

V. Parra-Vega
Mechatronics Division, CINVESTAV-IPN
AV. IPN 2508, Sn P. Zacatenco, México, D.F.,7300. México
vparra@cinvestav.mx

***Abstract*— Lots of constrained motion control schemes have been proposed for robots. However, since constrained motion demands fast tracking with smooth control, few of these schemes are convenient in practice for many tasks, such as hand-control, polishing, grinding, and assembly operations. In particular, adaptive control is quite slow due to its overparametrization, while first order sliding mode control cannot be implemented because its chattering. On the other hand, second order sliding mode control demands knowledge of upper bounds. Recently, to ameliorate these limitations, the theoretical framework and simulations, a synergetic combination of adaptive and second order sliding mode control has been proposed. This controller achieves simultaneous exponential convergence of position/force tracking errors with chattering-free control and without any knowledge of upper bounds. Then, it stands as a viable control technique that exhibits the best of adaptive and sliding mode control. In this paper, the real-time, Linux RTAI-based, experimental results of this controller is presented on a direct-drive robot manipulator equipped with six axis JR3 force sensor. Comparative results suggest its superior performance.**

***Index Terms*— Adaptive Control, Second Order Sliding Mode Control, Robot Manipulator, Constrained Motion.**

I. Introduction

Passivity-based force/position adaptive controllers with and without first order sliding mode control have been proposed in literature. Those ones based only on adaptive control, e.g. [5],[6], with no persistent excitation, present a slow performance due to system introduced chain of integrators and the parameter update, that is, only asymptotic convergence of position and force tracking errors can be achieved. On the other hand, the adaptive controllers based on first order sliding modes allow exponential convergence of position and force tracking errors, but the sliding mode introduces high frequency components, thus, it becomes impossible to implement in a real plant due to finite bandwidth of actuators.

Considering the above, Parra *et. al* ([1] $\sim$ [4]) proposed a controller able to simultaneously control both position and force variables with an effective combination of adaptive control and sliding mode control. The error coordinate representation induces a second order sliding mode and gives rise to a robust exponential convergence. The holonomic constraint is manipulated to derive two orthogonal subspaces of position-velocity and integral-of-force tracking errors. This way, the sliding modes arise on the tangential and normal subspaces at the contact point for all time. In the constrained motion case, orthogonalized sliding modes arises to ensure the exponential convergence of position and force tracking errors. The control structure can be seen as composed by two control loops: an outer adaptive control loop compensates for parametric uncertainty while an inner sliding mode control gives the missing energy to yield the exponential convergence robust performance. Since the second order sliding mode does not introduce high frequency components, then we have a continuous controller that can be implemented in a real plant.

A. Contribution

The contribution of this article is to validate experimentally the theoretical framework [2],[4] on a two degree-of-freedom direct-drive manipulator, provided with a six axis force sensor, interacting with a highly rigid surface. The control system is running over Linux-RTAI operating system.

B. Organization

The paper is organized as follows. In Section II, the system model and its properties are presented. Section III gives the proposed control law, while Section IV shows some remarks about the control scheme. The experimental setup is described in Section V, while experimental results are shown in Section VI. Finally, conclusions are drawn in Section VII.

II. Robot Dynamics

The dynamic model of a robot manipulator when the end-effector is in contact with an undeformable surface is given as follows

$$H(q)\ddot{q} + \{B_0 + C(q,\dot{q})\}\dot{q} + g(q) = \tau + J_{\varphi+}^T\lambda \quad (1)$$

$$\varphi(q) = 0 \quad (2)$$

where$H(q) \in \Re^{n\times n}$ denotes a symmetric positive definite inertial matrix, $B_0 \in \Re^{n\times n}$ stands for a diagonal positive definite matrix composed of damping friction coefficients for each joint, $C(q,\dot{q}) \in \Re^{n\times n}$ represents the Coriolis and centripetal torques, $g(q) \in \Re^n$ models the gravitational torques, $\tau \in \Re^n$ stands for the torque input, $\lambda \in \Re^r$ plays a role of the constrained Lagrangian representing the magnitude of the contact force (when $r = 1$ there is one contact point), $J_{\varphi+}^T = J_{\varphi+}^T(q) = J_{\varphi}^T(q)\left(J_\varphi(q)J_\varphi^T(q)\right)^{-1}$ stands for the normalized projection of the $J_\varphi(q) \in \Re^{1\times n}$ whose span is normal at the tangent plane that arises at the contact point and $J_\varphi(q) =$

$(\frac{\partial \varphi}{\partial q_1}, \frac{\partial \varphi}{\partial q_2}, \ldots, \frac{\partial \varphi}{\partial q_n})$ denotes the gradient of the object surface. The infinitely rigid surface is described by a geometric function $\varphi(q_1, \ldots, q_n) = \varphi^*(x_1, x_2, x_3, w_4, w_5, w_6) = 0 \in \Re^6$, where $x = (x_1, x_2, x_3)^T$ denotes the cartesian coordinates (task coordinates) fixed at the inertial reference frame, and $w = (w_4, w_5, w_6)^T$ its associated Euler angles. Clearly, an orthogonal projection of $J_\varphi(q)$ arises onto the tangent space at the contact point between the end-effector and the surface $\varphi(q) = 0$, as

$$Q(q) = I - J_{\varphi+}^T(q) J_\varphi(q)$$

where I denotes the $n \times n$ identity matrix. Therefore, while the manipulator is moving along the $p-dof$ on the constraint surface spanned by the image of $Q(q)$, there arises $Q(q)\dot{q} = \dot{q}$. Since both transformations $J_\varphi(q)$ and $Q(q)$ are orthogonal, we have the following useful properties: $i) J_\varphi(q)\dot{q} = 0$, $ii) Q(q) J_\varphi^T(q) = 0$ and, $iii) Q(q) J_{\varphi+}^T(q) = 0$. Now, equation (1) can be parametrized linearly in terms of a nominal reference $(\dot{q_r}, \ddot{q_r})^T \in \Re^{2n}$ as follows

$$H(q)\ddot{q_r} + \{B_0 + C(q, \dot{q})\}\dot{q_r} + G(q) = Y_r \Theta \tag{3}$$

where the regressor $Y_r = Y_r(q, \dot{q}, \dot{q_r}, \ddot{q_r}) \in \Re^{n \times m}$ is composed of known nonlinear functions, and $\Theta \in \Re^m$ is assumed to represent m unknown but constant physical robot parameters, with $(\dot{q_r}, \ddot{q_r})$ to be defined yet. Then, adding and subtracting (3) into (1), the open loop error equation arises, where arguments are omitted for simplicity

$$H\dot{S} = -(B_0 + C)S - Y_r\Theta + J_{\varphi+}^T \lambda + \tau \tag{4}$$

where the extended error $S = \dot{q} - \dot{q_r}$ carries out a change of coordinates through $(\dot{q_r}, \ddot{q_r})$. Let us now design $(\dot{q_r}, \ddot{q_r})$.

A. Change of coordinates

Consider

$$\begin{aligned} \dot{q_r} = Q\{\dot{q_d} - \sigma\Delta q + S_{dp} - \gamma_1 \int_{t_0}^{t} sgn(S_{qp}(\varsigma))d\varsigma\} \\ + \beta J_\varphi^T\{\Delta F - S_{dF} + \gamma_2 \int_{t_0}^{t} sgn(S_{qF}(\varsigma))d\varsigma\} \end{aligned} \tag{5}$$

where $\Delta q = q - q_d$, $\Delta F = \int_{t_0}^{t}(\lambda - \lambda_d)(\varsigma)d\varsigma$, $\sigma, \gamma_1 \in \Re_+^{n \times n}$ and $\beta, \gamma_2 > 0$. The subscript "d" denotes the desired reference values, and $sgn(x)$ stands for the discontinuous signum function of x. Substituting (5) into $S = \dot{q} - \dot{q_r}$ gives rise to

$$S = QS_{vp} - \beta J_\varphi^T S_{vF} \tag{6}$$

where the orthogonal extended position and force manifolds S_{vp} and S_{vF}, respectively, are defined by

$$S_{vp} = S_{qp} + \gamma_1 \int_{t_0}^{t} sgn(S_{qp}(\varsigma))d\varsigma \tag{7}$$

$$S_{vF} = S_{qF} + \gamma_2 \int_{t_0}^{t} sgn(S_{qF}(\varsigma))d\varsigma \tag{8}$$

with the following definitions

$$\begin{array}{ll} S_{qp} = S_p - S_{dp} & S_{qF} = S_F - S_{dF} \\ S_p = \Delta\dot{q} + \sigma\Delta q & S_F = \Delta F \\ S_{dp} = S_p(t_0)e^{-\kappa_1(t-t_0)} & S_{dF} = S_F(t_0)e^{-\kappa_2(t-t0)} \end{array} \tag{9}$$

where $\kappa_1, \kappa_2 > 0$. Using (5) and its derivative into (3), the open loop error equation (4) becomes

$$H\dot{S} = -(B_0 + C)S + \tau + J_{\varphi+}^T\lambda - Y_{cont}\Theta - \xi \tag{10}$$

where $\xi = H(Q\gamma_1 Z_1 - \beta J_\varphi^T \gamma_2 Z_2)$ stands as a bounded discontinuous term, and $Y_{cont} = Y_r(q, \dot{q}, \dot{q}_r, \ddot{q}_{cont})$ is continuous as follows

$$\begin{aligned} \ddot{q}_{cont} = \dot{Q}\{\dot{q_d} - \sigma\Delta q + S_{dp} - \gamma_1 \int_{t_0}^{t} sgn(S_{qp})\} \\ + Q\{\ddot{q_d} - \sigma\Delta\dot{q} + \dot{S}_{dp} - \gamma_1 tanh(\alpha_1 S_{qp})\} \\ + \beta\dot{J}_\varphi^T\{\Delta F - S_{dF} + \gamma_2 \int_{t_0}^{t} sgn(S_{qF})\} \\ + \beta J_\varphi^T\{\Delta\dot{F} - \dot{S}_{dF} + \gamma_2 tanh(\alpha_2 S_{qF})\} \end{aligned} \tag{11}$$

and

$$\begin{aligned} Z_1 = tanh(\alpha_1 S_{qp}) - sgn(S_{qp}) \\ Z_2 = tanh(\alpha_2 S_{qf}) - sgn(S_{qF}) \end{aligned}$$

$\tanh(x)$ is the hyperbolic tangent function of (x), and $\alpha_1, \alpha_2 > 0$ are constants. Notice that Z_1, Z_2 are discontinuous, but bounded and have the following useful properties near the origin for subsequent stability analysis $Z_{1,2} \leq +1, Z_{Sqp, SqF \to 0_-} = +1$ $Z_{1,2} \geq -1, Z_{Sqp, SqF \to 0_+} = -1$.

Remark 1. GETTING RID OF DISCONTINUITIES. The manipulation over $\ddot{q}_r$ is obligated to avoid introducing any high frequency components, that is the computation of $\ddot{q}_r$ becomes

$$\begin{aligned} \ddot{q}_r = Q\{\ddot{q}_d - \sigma\Delta\dot{q} + \dot{S}_{dp} - \gamma_1 sgn(S_{qp}(\varsigma))d\varsigma\} \\ + \dot{Q}\{\dot{q_d} - \sigma\Delta q + S_{dp} - \gamma_1 \int_{t_0}^{t} sgn(S_{qp}(\varsigma))d\varsigma\} \\ + \beta J_\varphi^T\{\Delta\dot{F} - \dot{S}_{dF} + \gamma_2 sgn(S_{qF}(\varsigma))d\varsigma\} \\ + \beta\dot{J}_\varphi^T\{\Delta F - S_{dF} + \gamma_2 \int_{t_0}^{t} sgn(S_{qF}(\varsigma))d\varsigma\} \end{aligned} \tag{12}$$

thus

$$H\ddot{q_r} + \{B_0 + C(q, \dot{q})\}\dot{q_r} + G = Y_{cont}\Theta + H\rho \tag{13}$$

with $\rho = (Q\gamma_1 Z_1 - \beta J_\varphi^T \ \gamma_2 Z_2)$. This separates all discontinuous, but bounded, signals to be casted as disturbances ξ in (10). In this way, the controller τ does not have to deal with the discontinuous regressor (12), but with the continuous regressor (11).■ Now we are ready to present the main result.

III. Adaptive second order sliding mode control

Consider the following continuous control law

$$\tau = -K_d S + Y_{cont}\hat{\Theta} + J_{\varphi+}^T\{\eta\gamma_2 \int_{t_0}^{t} sgn(S_{qF})\} + J_{\varphi+}^T\{-\lambda_d + \eta\Delta F + \gamma_2 tanh(\alpha_2 S_{qF})\}$$
$$\dot{\hat{\Theta}} = -\Gamma Y_{cont}^T S \quad (14)$$

for $K_d = K_+^T \in R^{n\times n}$, $\Gamma = \Gamma_+^T \in R^{m\times m}$, and $\hat{\Theta}$ stands for the online estimation of the unknown parameters Θ. We now have the following.

Theorem. Consider a constrained robot manipulator (1)-(2) in closed-loop with the given control law (14). Then, the robotic system yields a second order sliding mode regime with local exponential convergence for position errors and global exponential convergence for force errors under robot parametric uncertainty.

Proof. An outline of the proof can be found in appendix.

IV. Remarks

Remark 2. How to tune feedback gains: γ_i. Since γ_i $(i = 1, 2)$ depends on the norm of the derivative of the state it is difficult to know a *priori* its value to induce a sliding mode. Suppose γ_i is set to zero, in which case our controller renders asymptotic stability (the controller collapses into [5] if $S_{dp}, S_{dF} = 0$). Constants γ_i can be increased gradually until sliding modes arise. Note that this is not a high gain result since larger γ_i do not mean a larger domain of stability. Nevertheless, γ_i is small because the outer adaptive control loop compensates for disturbances ξ. ■

Remark 3. No persistent excitation condition: Most of the adaptive controllers that attain exponential stability rely on the persistent excitation condition of the regressor. Note, that we have not assumed such condition. ■

Remark 4. Robustness:. Parametric uncertainty is compensated via the adaptive control loop and robust exponential convergence is achieved via sliding mode, with smooth and chattering free control signals. ■

Remark 5. The integral term: The integral term in S plays the role of compensating dynamically the effect of parametric disturbances in terms of S_{vp} and S_{vF}. This integral term and $tanh(\alpha_2 S_{qF})$ are the key of the whole algorithm. ■

Remark 6. Finite time convergence: Since sliding mode exists for all time, the state is trapped into a lower order manifold, which is invariant to system dynamics and robot parameters, that is

$$S_{qp} = 0 \forall t \rightarrow S_p = S_{dp} \rightarrow \Delta\dot{q} = -\sigma\Delta q + S_p(t_0)e^{-\kappa_1(t-t_0)}$$
$$S_{qF} = 0 \forall t \rightarrow S_F = S_{dF} \rightarrow \Delta F = S_F(t_0)e^{-\kappa_2(t-t_0)}$$

Surprisingly, the above equations govern the closed-loop sliding dynamics of the closed-loop trajectories, producing exponential convergence. On the other hand, it is still possible to converge faster. It is possible to attain finite time convergence of position tracking errors by means of well-posed terminal attractors. Finite time convergence can be tuned arbitrarily via a time-varying gain $\sigma(t)$ so as to drive smoothly $\Delta q(t)$ toward its equilibrium $\Delta q(t) = 0$. Gain $\sigma(t)$ is tailored with a Time Base Generator (TBG), which may be a fifth order polynomial that smoothly goes from $0 \rightarrow 1$. For more details see [4] and [9]. ■

Remark 7. Versus adaptive and first order sliding mode: The proposed control scheme yields the adaptive controller when $\gamma_1, \gamma_2, S_{dp}, S_{dF}$ are zero. In this case, the closed loop system produces smooth control with slow trajectories. On the other hand, when $\tanh(\cdot)$ is substituted by $sgn(\cdot)$, it produces first order discontinuous sliding modes, which is only of academic interest, since there is not motor that can commute at such high frequency, due to the finite inertia of its rotor. ■

V. Experimental Station

Robot parameters and constant gains used in the experiments are shown in Table 1, and a photograph of the experimental setup is depicted in Fig. 2.

TABLE I
Dimension parameters (*Par*) of the robot arm, and feedback gains.

Par	Value	Gain	Value	Gain	Value
m_1	6.72 Kg	K_d	$diag$(20,1.65)	β	0.1
m_2	2.03 Kg	γ_1	$diag$(0.1)	γ_2	0.01
l_1	0.4 m	σ	$diag$(5)	η	0.3
l_2	0.3 m	Γ	$diag$(0.001)	κ_1, κ_2	20

Fig. 1. Dimension parameters (*Par*) of the robot arm, and feedback gains.

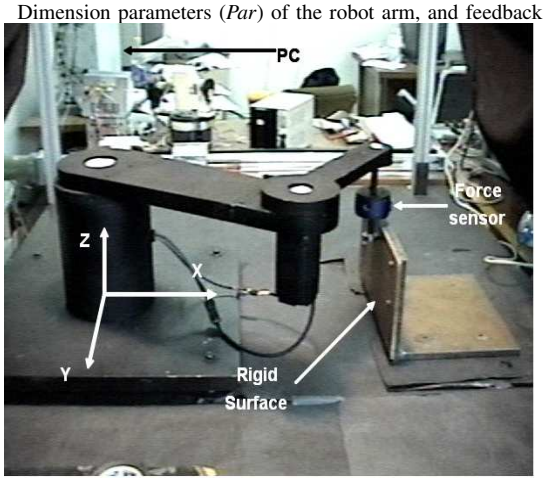

Fig. 2. Experimental setup.

A. The Hardware

A 2-dof arm is integrated using aluminum A60 for the whole mechanical structure. Direct-drive Yaskawa AC servomotors SGM-08A314 and SGM-04U3B4L with 2048 pulse

encoders are directly coupled to the links. Digital drive electronics from the Yaskawa servopacks (SGD-08AS and SGDA-04AS for each motor, respectively) are integrated through some additional custom made optoelectronic circuits to yield additional isolated coupling. A six-axis force-moment sensor 67M25A-I40-200N12 by JR3 Inc., provided with a DSP Based Interface System for PCI bus, is mounted at the end effector of the robot. The sensor has a maximum rating of $\pm 200N$ in the XY axes and twice in the Z axis. While the arm is in free motion the actual environmental electronic noise in the force sensor readings in the range of $0.1N - 0.5N$. The tool used in the experiments is a rigid aluminum probe with a bearing in its tip, implanted to reduce contact friction, as shown in Fig. 3. The robot task is to move its tool-tip along a specified trajectory over the steel surface while at the same time exerts a specified profile of force normal to the surface.

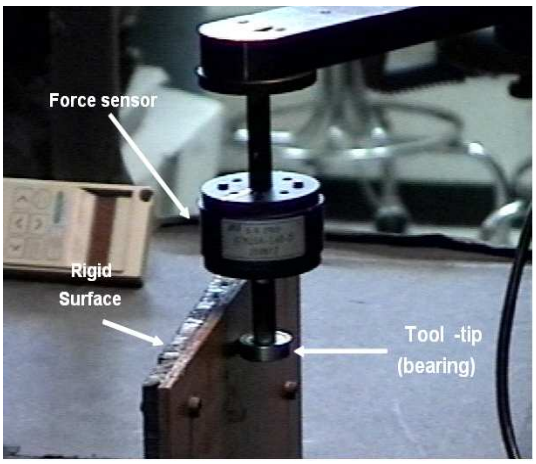

Fig. 3. Rigid aluminum tool-tip.

B. The firmware and software

The control system is running in real-time with a sampling rate of 1 KHz on a PC over Linux-RTAI operating system. Low level programming provides the interface to a Sensoray 626 I/O card which contains internal quadrature encoder interface, 14 bit resolution analog outputs and digital I/O. Velocity is computed using a dirty Euler numerical differentiation formula filtered with a lowpass second order Butterworth filter, with a cutoff frecuency of 20Hz.

VI. Results

The robot is initialized with a high gain PD since the parametric uncertainty is 100%. The inertial frame of the whole system is at the base of the robot and the contact surface is at $x = 0.495\ m$ rendering a YZ plane. The experiment is performed as follows (see Fig. 4):

1) From $t = 0\ s$ to $t = 5\ s$, the end effector is requested to move, in free motion, from its initial condition until it makes contact with the surface. The end effector lasts 2 more seconds (from 5 to 7 seconds)
2) From time $t = 7\ s$ to $t = 18\ s$ the tool-tip exerts a desired profile of force normal to the surface (0 to 5 N) while moving along Y axis from 0.1 to -0.03 m
3) From $t = 18\ s$ to $t = 28\ s$ the exerted force is incremented from 5 to 7.5 Newtons, while moving along Y axis from -0.03 to 0.1 m, as can be seen in Fig. 6 and Fig. 7.

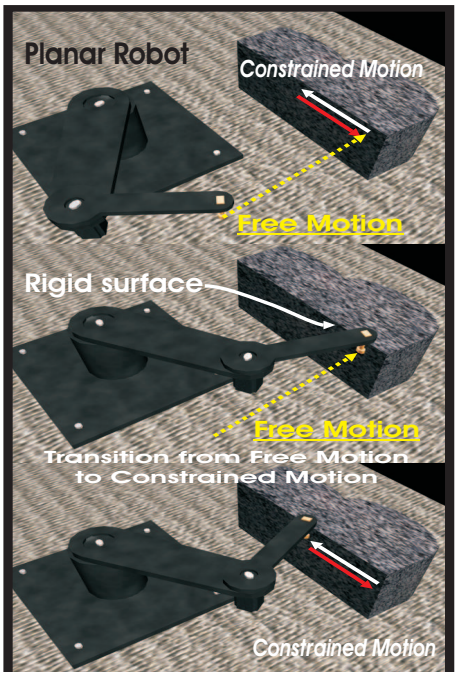

Fig. 4. The desired task.

Both desired position and force are designed with $\Phi(t) = P(t)\left[\mathbf{X}_f - \mathbf{X}_i\right] + \mathbf{X}_i$, where $P(t)$ is a fifth order polynomial that satisfy $P(t_i) = 0, P(t_f) = 1$ and $\dot{P}(t_i) = \dot{P}(t_f) = 0$. The subscript *'i'* and *'f'* denote *initial* and *final* stages, respectively. At the first stage of the experiment, the control law (14) is used with the force part set to zero, i.e. $J_\varphi^T = 0$ and $Q = I$. It is rather easy to prove that this scheme is stable for unconstrained motion. Once the tool-tip is in contact with the surface the control force term is switched on. Fig. 5 shows the input torques. It can be observed that there are not saturation problems and the smooth behavior. Fig. 7 depicts the real and desired trajectories in the cartesian plane. The results for the tracking errors can be seen in Fig. 8 for joint coordinates and in Fig. 9 for Cartesian coordinates. As a comparison with the proposed controller, it is presented the experimental results of an Adaptive force/position control. The adaptive control is easily obtained considering Remarks 2 and 7.

VII. Conclusions

A fast trajectory tracking and smooth controller is experimentally validated. It is argue that such stability properties are very convenient to constrained motion tasks, in particular, when there is contact to rigid objects. The adaptive controller is designed over a second order sliding mode

error coordinate system to attain exponential convergence, and enhanced parameter stability. This result represents a systematic combination of model-based adaptive control and chattering-free sliding mode control for constrained motion robots. Experimental results validate the predicted theoretical performance. Worth to mention is that the system stability remains even when the robot end-effector motion switches from free motion to constrained motion due to its passivity properties, under a set of conditions [10]. Experimental results comply dully to the theoretical stability properties.

APPENDIX

The formal proof ([2]) firstly proves that all closed loop signals are bounded, using the following Lyapunov function

$$V = \frac{1}{2}(S^T H S + \beta S_{vF}^T S_{vF} + \Delta\Theta^T \Gamma^{-1} \Delta\Theta) \tag{15}$$

for scalar $\beta > 0$, and $\Delta\Theta = \Theta - \hat{\Theta}$ produces the total derivative of Lyapunov

$$\begin{aligned}
\dot{V} &= -S^T(K_d + B_0)S - \beta\eta S_{vF}^T S_{vF} \\
&\quad - S^T H Q \gamma_1 Z_1 + S^T H \beta J_\varphi^T \gamma_2 Z_2 \\
&\leq -S^T K_d S - \beta\eta S_{vF}^T S_{vF} \\
&\quad + \gamma_1 \|S^T H Q\| + \beta\gamma_2 \|S^T H J_\varphi^T\| \\
&\leq -S^T K_d S - \beta\eta S_{vF}^T S_{vF} \\
&\quad + \gamma_1 \|H\| \|Q\| \|S\| + \beta\gamma_2 \|H\| \|J_\varphi^T\| \|S\| \\
&\leq -S^T K_d S - \beta\eta S_{vF}^T S_{vF} + \epsilon_1 \|S\| + \epsilon_2 \|S\|
\end{aligned} \tag{16}$$

Thus, if K_d, β and η are large enough such that S converges into a neighborhood $\epsilon = f_1(\epsilon_1) + f_2(\epsilon_2) > 0$ centered in the equilibrium $S = 0$, namely

$$S \to \epsilon \quad as \quad t \to \infty$$

This result stands for local stability of S provided that the state is near the desired trajectories for any initial condition, and that $\Delta\Theta \in \mathcal{L}_\infty$. This boundedness leads to the existence of the constants $\epsilon_3 > 0$ and $\epsilon_4 > 0$ such that

$$|\dot{S}_{vp}| < \epsilon_3, \tag{17}$$

$$|\dot{S}_{vF}| < \epsilon_4 \tag{18}$$

where $|X|$ stands for $\sum_{i=1}^{n} |X_i|$.

Secondly, it proves that sliding modes, and therefore exponential tracking, are induced. It follows that if we multiply the derivative of S_{qp} in (7) by S_{qp}^T, we obtain

$$\begin{aligned}
S_{qp}^T \dot{S}_{qp} &= -\gamma_1 |S_{qp}| + S_{qp}^T \dot{S}_{vp} \\
&\leq -\gamma_1 |S_{qp}| + |S_{qp}||\dot{S}_{vp}|
\end{aligned} \tag{19}$$

Substituting (17) into (19) yields

$$S_{qp}^T \dot{S}_{qp} \leq -(\gamma_1 - \epsilon_3)|S_{qp}| \tag{20}$$

where γ_1 must be chosen such that $\gamma_1 > \epsilon_3$. The equation (20) is precisely the condition for the existence of a sliding mode at $S_{qp}(t) = 0$ [8]. The sliding mode is established in a time $t \leq |S_{qp}(t_0)|/(\gamma_1 - \epsilon_3)$ and, according to (9), $S_{qp}(t_0) = 0$ implies that $S_{qp}(t) = 0\ \forall t$, therefore the position tracking converge exponentially towards the desired trajectory $q_d(t)$. Similarly, i f we multiply the derivative of S_{qF} in (8) by S_{qF}^T, we obtain

$$S_{qF}^T \dot{S}_{qF} = -\gamma_2 |S_{qF}| + S_{qF}^T \dot{S}_{vF} \leq -\gamma_2 |S_{qF}| + |S_{qF}||\dot{S}_{vF}| \tag{21}$$

substituting (18) into (21) yields

$$S_{qf}^T \dot{S}_{qf} \leq -(\gamma_2 - \epsilon_4)|S_{qf}| \tag{22}$$

where γ_2 must be chosen such that $\gamma_2 > \epsilon_4$. The equation (22) is precisely the condition for the existence of a sliding mode at $S_{qF}(t) = 0$ [8]. The sliding mode is established in a time $t \leq |S_{qF}(t_0)|/(\gamma_2 - \epsilon_4)$ and, according to (9), $S_{qF}(t_0) = 0$ implies that $S_{qF}(t) = 0\ \forall t$, which implies that $\lambda \to \lambda_d$ exponentially fast. ■

REFERENCES

[1] V. Parra-Vega and S. Arimoto, "Adaptive Control for Robot Manipulators with Sliding Mode Error Coordinate System: Free and Constrained Motions", *Proc. IEEE Int. Conf. on Rob. and Autom.*, pp. 591-596, 1995.

[2] V. Parra-Vega and S. Arimoto, "A Passivity-based Adaptive Sliding Mode Position-Force Control for Robot Manipulators", *Int.Journal of Adaptive Control and Signal Processing*, Vol. 10, pp. 365-377, 1996.

[3] Y. H. Liu, V. Parra-Vega, and S. Arimoto, "Decentralized Adaptive Control Of Multiple Manipulators in Cooperation", *Int. Journal of Control*, Vol. 67, No. 5, pp. 649-673, 1997.

[4] V. Parra-Vega, A. Castillo-Tapia, L.G. García-Valdovinos, and M.A. Arteaga-Pérez, "Adaptive Second Order Sliding Mode Control for Finite-Time Tracking of Constrained Robot Manipulators", *Congreso Latinoamericano de Control Automático CLCA'02*, Guadalajara, México, 2002.

[5] L.L. Whitcomb and S. Arimoto, "Adaptive Model-Based Hybrid Control of Geometrically Constrained Robot Arms", *IEEE Trans. on Robotics and Automation*, Vol. 9, Issue 1, pp. 105-116, Feb. 1997.

[6] Y.-H. Liu, K. Kitagaki, T. Ogasawara, and S. Arimoto, "Model-Based Adaptive Hybrid Control for Manipulators Under Multiple Geometric Constraints", *IEEE Trans. on Control Systems Technology*, Vol. 7, No. 1, Jan., 1999.

[7] Spong, M. W. and Vidyasagar, M., Robot Dynamics and Control

[8] V. Utkin, "Variable Structure Systems: Control and Optimization", *Springer-Verlag*, 1992.

[9] V. Parra-Vega, "Second Order Sliding Mode Control for Robot Arms with Time Base Generators for Finite-Time Tracking", *Dynamics and Control*, 11, 175-186, 2001.

[10] P. Akella, V. Parra-Vega., Arimoto S. and T. Tanie, "Discontinuous Adaptive Control for Robot Manipulators Executing Free and Constrained Tasks ", *Proc. of the IEEE Robotics and Automation*, San Diego (1994), pages 3000-3007.

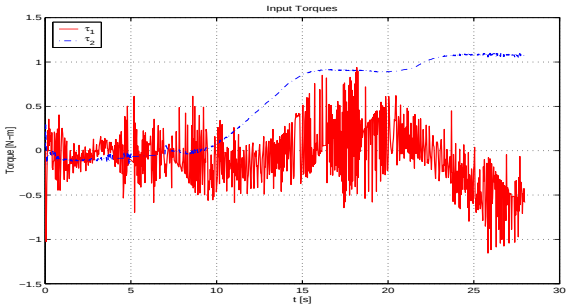

Fig. 5. Control inputs.

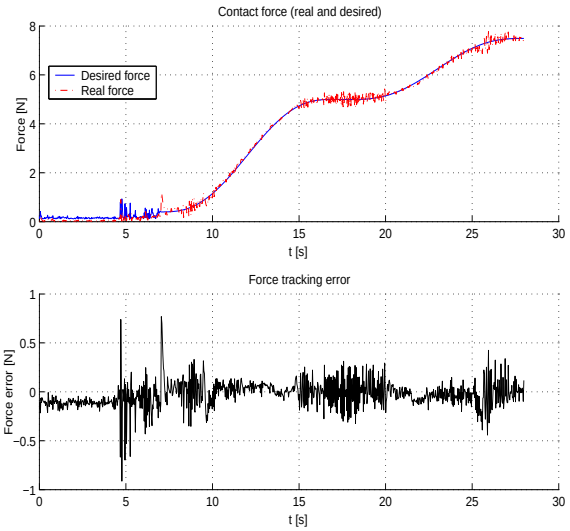

Fig. 6. End effector force.

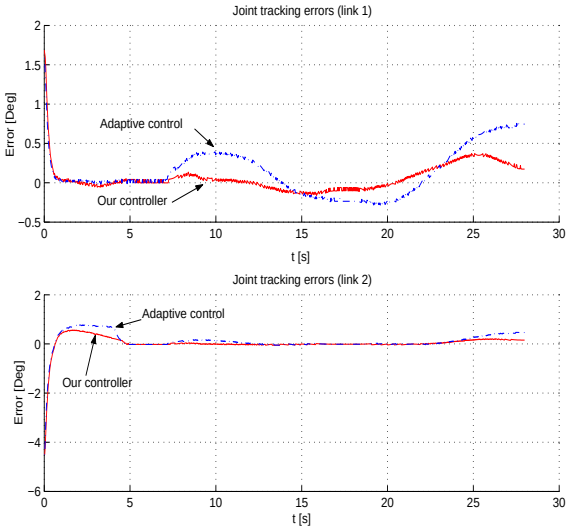

Fig. 8. Tracking errors in joint coordinates.

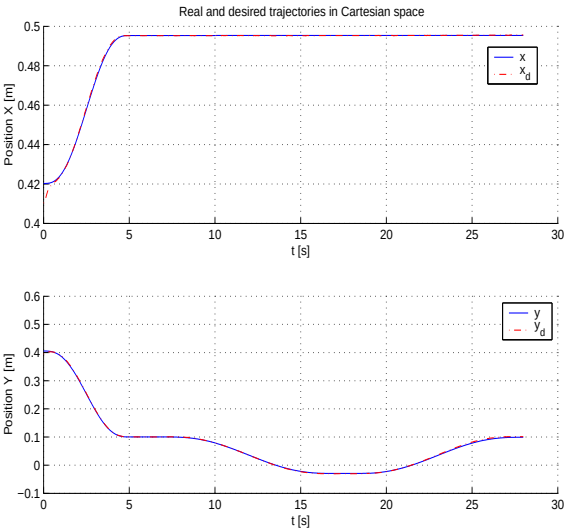

Fig. 7. Trajectories in Cartesian space.

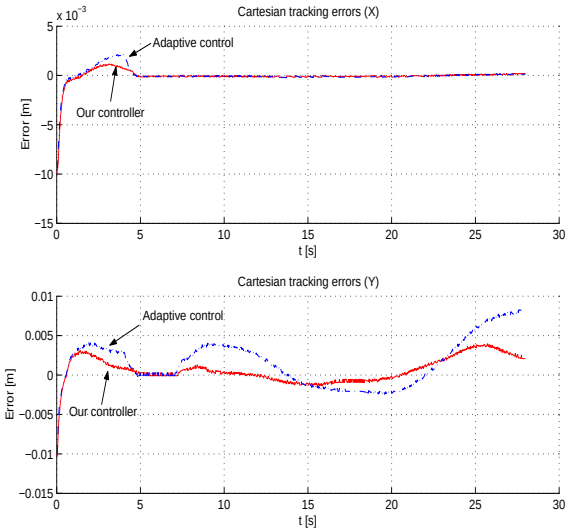

Fig. 9. Tracking errors in Cartesian coordinates.